

SCIENTIFIC REPORTS



OPEN

Size-controllable Ni₅TiO₇ nanowires as promising catalysts for CO oxidation

Yanan Jiang¹, Baodan Liu¹, Lini Yang², Bing Yang¹, Xiaoyuan Liu¹, Lusheng Liu¹, Christian Weimer³ & Xin jiang¹

Received: 06 May 2015

Accepted: 25 August 2015

Published: 23 September 2015

Ni₅TiO₇ nanowires with controllable sizes are synthesized using PEO method combined with impregnation and annealing at 1050°C in air, with adjustment of different concentrations of impregnating solution to control the dimension of nanowires. The resulting nanowires are characterized in details using X-ray diffraction, scanning electron microscopy, transmission electron microscopy and energy dispersive X-ray analysis. In addition, the CO catalytic oxidation performance of the Ni₅TiO₇ nanowires is investigated using a fixed-bed quartz tubular reactor and an on-line gas chromatography system, indicating that the activity of this catalytic system for CO oxidation is a strong dependency upon the nanocrystal size. When the size of the Ni₅TiO₇ nanowires is induced from 4 μm to 50 nm, the corresponding maximum conversion temperature is lowered by ~100 °C.

The climate debate in the context of exhaust pollution has been paid extensive attention worldwide for many years because of jeopardizing human health, especially the CO emission from automobile exhaust and incomplete combustion of hydrocarbons has been regarded as a major problem^{1,2}. As a result, the CO conversion and removal using efficient catalysts has been a hot topic either in fundamental research or industrial applications. Over the past decades, metal oxide compounds decorated with noble metal particles such as Pt/SnO₂, Pd/SnO₂, Au/TiO₂ etc have been demonstrated to be efficient catalysts for CO oxidation^{3,4}. However, the limited resource and high cost of noble metals promote us to search for alternative peers with comparable catalytic capability and commercially available low-cost. With this demand, extensive efforts are being focused on the developing of highly efficient and stable, but cost down metal oxide catalysts free of noble metal decorations for CO oxidation.

So far, research on transition metal oxides as catalysts for CO oxidation has made significant progress based on the combination of different metal compound oxides. For example, some composite metal oxides such as CuO_x/CeO₂, CoO_x/Al₂O₃, MnO_x/Al₂O₃, Ce_{1-x}Ti_xO₂, Ce_{0.8}Zr_{0.2}O₂ have been identified as good catalysts for CO oxidation⁵⁻⁹. It's well known that the catalytic activity of transition metal oxides is strongly dependent on some key factors such as well-defined facets, size, morphology, composition and crystallinity. Especially, the smaller size directly results in the huge increase of specific surface area and active sites on the surface and thus leads to amazing performance enhancement^{10,11}. Therefore, it is quite essential to develop a facile approach for producing transitional metal oxide catalysts with large yield, controllable size and dimension, tunable catalysis performance and low cost considering the future industrial application. In contrast to conventional popular methods for synthesizing transition metal oxides, for example, chemical vapour deposition (CVD)¹², solvothermal synthesis¹³, and hydrothermal synthesis¹⁴, the innovation approach of Plasma Electrolytic Oxidation (PEO) has been demonstrated extremely successful and efficient in producing porous MO_x/TiO₂/Ti oxide nanostructures (where M = Ni, Cu, Mn,

¹Shenyang National Laboratory for Materials Science, Institute of Metal Research (IMR), Chinese Academy of Sciences (CAS), No. 72 Wenhua Road, Shenyang 110016 China. ²College of Chemistry, Liaoning University, Shenyang, Liaoning, 110036, China. ³Institute of Materials Engineering, University of Siegen, Paul-Bonatz-Straße 9-11, Siegen, 57076 Germany. Correspondence and requests for materials should be addressed to B.L. (email: baodanliu@imr.ac.cn) or X.J. (email: xjiang@imr.ac.cn)

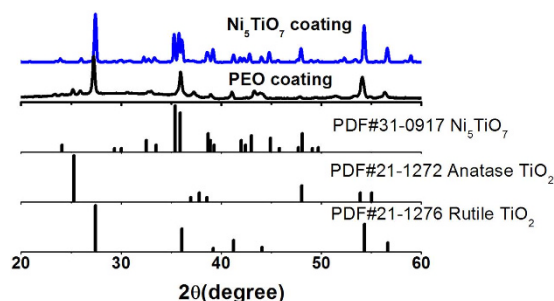


Figure 1. XRD patterns of PEO coating and Ni_5TiO_7 layer after annealing at 1050°C for 1 hour; Standard XRD data of Ni_5TiO_7 , anatase TiO_2 and rutile TiO_2 are also shown as references.

W, Co) and $(\text{CeO}_x, \text{ZrO}_2)/\text{TiO}_2/\text{Ti}$ coatings¹⁵, with its obvious advantages of an easy operation, low-cost and versatility in dimension controlling and composition tailoring¹⁶.

Ni_5TiO_7 , a promising catalyst for tar conversion, was first synthesized with flux method by Fumio Shimura and Tsutomu Kawamura in 1976^{17,18}. It possesses an orthorhombic symmetry with a unit cell lattice constants $a = 9.20 \pm 0.02 \text{ \AA}$, $b = 2.99 \pm 0.01 \text{ \AA}$ and $c = 12.17 \pm 0.04 \text{ \AA}$ ¹⁷. The structural formula of Ni_5TiO_7 can be simply regarded as the combination of NiO and TiO_2 with a stoichiometric ratio of $\text{NiO}:\text{TiO}_2 = 5:1$ (or $\text{Ni}:\text{Ti}:\text{O} = 5:1:7$). However, the formation of Ni_5TiO_7 crystal cannot be achieved by simply heating the NiO and TiO_2 powders at high temperature. Until very recently, Jiang and his co-workers in Siegen University (Germany) reported the fabrication of nanostructured Ni_5TiO_7 catalyst using PEO method and demonstrated its outstanding performance in biomass gasification process¹⁸. However, no further work regarding to the size controlling of Ni_5TiO_7 nanocatalyst, which is crucial for understanding its nucleation, crystallization and further catalytic performance improvement, was preceded. In addition, exploring its multi-functions in environment-related issues and long-term stability is still essential for considering its future practical applications in environment processing.

In this context, the size controlling of Ni_5TiO_7 catalysts fabricated by PEO method is systemically investigated through tailoring the concentration of Ni ion in impregnation solutions. The morphology and size evolution of Ni_5TiO_7 nanostructures as a dependence of Ni ions are also discussed. As a key part, the CO catalytic oxidation behaviour of the as-prepared Ni_5TiO_7 nanowires used as catalysts is also evaluated for exploring their promising applications in CO conversion. In addition, the size influence of Ni_5TiO_7 catalysts on their CO catalytic efficiency and the stability at high temperature are also studied. It is demonstrated that the nanoscaled Ni_5TiO_7 catalysts with huge surface area and excellent crystallinity exhibit broad application potential and incomparable advantage in CO oxidation and biomass gasification, especially in car exhaust processing or the degradation of waste gas pollutions, for the sake of their high catalytic performance, low cost and easy preparation process.

Results and Discussion

X-ray diffraction (XRD) is first used to examine the crystalline structures and phase purities of as-synthesized samples obtained at PEO stage and subsequent annealing. Figure 1 shows the XRD patterns of PEO coating and its subsequent dipping into 0.5 M $\text{Ni}(\text{NO}_3)_2$ solution and annealing at 1050°C . It is found that mixed anatase and rutile TiO_2 phases have been directly formed in PEO coating after the arc-discharging process in electrolyte. The peak from Ti substrate is not observed because of the excessive thickness of PEO coating ($\sim 10 \mu\text{m}$). In addition, a dome peak in the range of $20\text{--}40^\circ$ is also observed, which indicates the formation of some amorphous phase. After dipping the PEO coating in $\text{Ni}(\text{NO}_3)_2$ solution for 1 hour and heated at 1050°C , Ni_5TiO_7 phase with good crystallinity appears in the surface of the PEO coating and shows predominant diffraction intensity (Fig. 1), in good agreement with the standard structure data of Ni_5TiO_7 crystal (No. JCPDS: 31-0927). Meanwhile, the preformed anatase TiO_2 phase has completely disappeared from the PEO coating and only rutile TiO_2 phase is maintained due to the metastable feature of anatase TiO_2 at a critical phase transition temperature in the range of $400\text{--}1050^\circ\text{C}$.²³ The formation of Ni_5TiO_7 phase implies that Ni ions incorporated into porous PEO surface/matrix have reacted with Ti/ TiO_2 at high temperature.

Figure 2 shows the morphologies and compositions of the PEO coating and the as-synthesized Ni_5TiO_7 nanostructures annealed at 1050°C . It's found that the PEO coating with a thickness of $10 \mu\text{m}$ has a rough morphology with concaved pores uniformly distributing on the surface (Fig. 2a,b). The pores are formed during micro-arc discharging under high voltage and high surface temperature, which produces reduplicate melt and solidification reactions on Ti surface. Composition analysis performed on the PEO coating shows that the layer is mainly made of Ti and O elements (TiO_2) with Ni, P and W etc as minorities (Fig. 2c), indicating the formation of porous TiO_2 film. These Ni, P and W elements are directly from the electrolytes we used (see experimental section). The detection of Ni etc elements in the PEO coating suggests that the amorphous phase corresponding to the broad dome in XRD

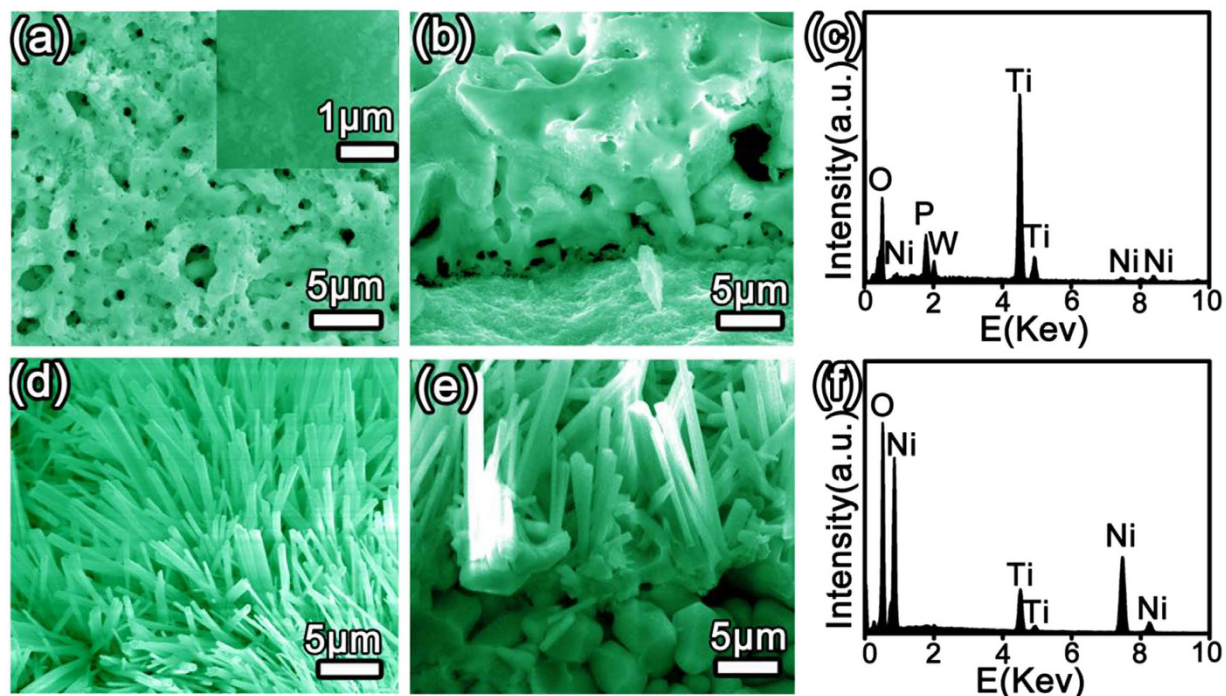


Figure 2. (a,b) SEM surface and cross-sectional morphologies of PEO coating; (d,e) SEM surface and cross-sectional morphologies of Ni_5TiO_7 grown on PEO coating at 1050°C ; (c,f) EDS results of PEO coating and Ni_5TiO_7 , respectively.

pattern (Fig. 1) may be assigned to some Ni-containing compound. To obtain Ni_5TiO_7 nanocrystals, the porous PEO coating dipped into $\text{Ni}(\text{NO}_3)_2$ solution is annealed at 1050°C for 1 hour, and it is found that needle-like nanowires with diameters ranging from 100 nm to $1\ \mu\text{m}$ are densely covered on the PEO coating surface (Fig. 2d). Cross-section SEM observation presented in Fig. 2e clearly shows that these nanowires are directly grown from the top layer of the porous coating and are tightly combined with the coating. In contrast to the predominant Ti and O constituents in initial PEO coating, the chemical compositions detected from the local nanowires are identified as Ni, Ti and O with a stoichiometric ratio close to Ni_5TiO_7 (Fig. 2f), further demonstrating the formation of Ni_5TiO_7 phase after high-temperature annealing.

Figure 3a shows a representative TEM image of Ni_5TiO_7 nanowires transferred from the porous TiO_2 coating. The smoothness of nanowire surface and the uniformity of nanowire diameter in the range of 200–500 nm can be clearly confirmed. No particles in nano-scaled size can be found at the nanowire surface and tip-end. Careful EDS analyses performed on different positions of the nanowire conclude that the nanowires are indeed made of Ni, Ti and O with an atomic ratio of Ni:Ti:O = 5:1:7 (Fig. 3b and Fig. S1), matching well with the composition value of standard Ni_5TiO_7 crystal. The Cu peak with negligible signal is directly from the Cu TEM grid for supporting the samples. Absence of any other impurity peak related to P and W elements that are introduced during PEO process demonstrates again the high phase and chemical purity of Ni_5TiO_7 nanowires. The high-temperature annealing of PEO coating at 1050°C in ambient environment only leads to the nucleation and crystallization of Ni_5TiO_7 phase and does not introduce any possible contamination. The superior crystallinity of Ni_5TiO_7 nanowires, proved by the succinct selective area electron diffraction (SAED) pattern (Fig. 3c) and HRTEM data (Fig. 3d), verify the single crystalline nature of Ni_5TiO_7 nanowires. The separated and periodic diffraction spots and well-aligned atom ordering confirm that Ni_5TiO_7 nanowires prepared by PEO method are free of structural defects like microtwins and stacking faults, indicating the obvious advance of this technique in the crystallinity controlling in comparison with other methods for metal oxide nanostructure preparation¹⁹. The lattice distance between two adjacent lattice planes parallel and perpendicular to the growth direction are measured to be 0.44 nm and 0.29 nm, respectively, matching well with the d-spacing value of (200) and (010) planes of orthorhombic Ni_5TiO_7 crystal. The growth orientation of Ni_5TiO_7 nanowires, along [010] direction, can also be confirmed as a result of a strong growth competition of the (010) surface against other low-indexed planes of the side facets. In addition, an outer layer with a thickness of few nanometers can be found on the surface of the Ni_5TiO_7 nanowire.

In the synthesis of Ni_5TiO_7 nanowires, it is found that Ni ions in the impregnation solution play a key role in organizing the initial nucleation locations and are essential for the nucleation (or growth) density

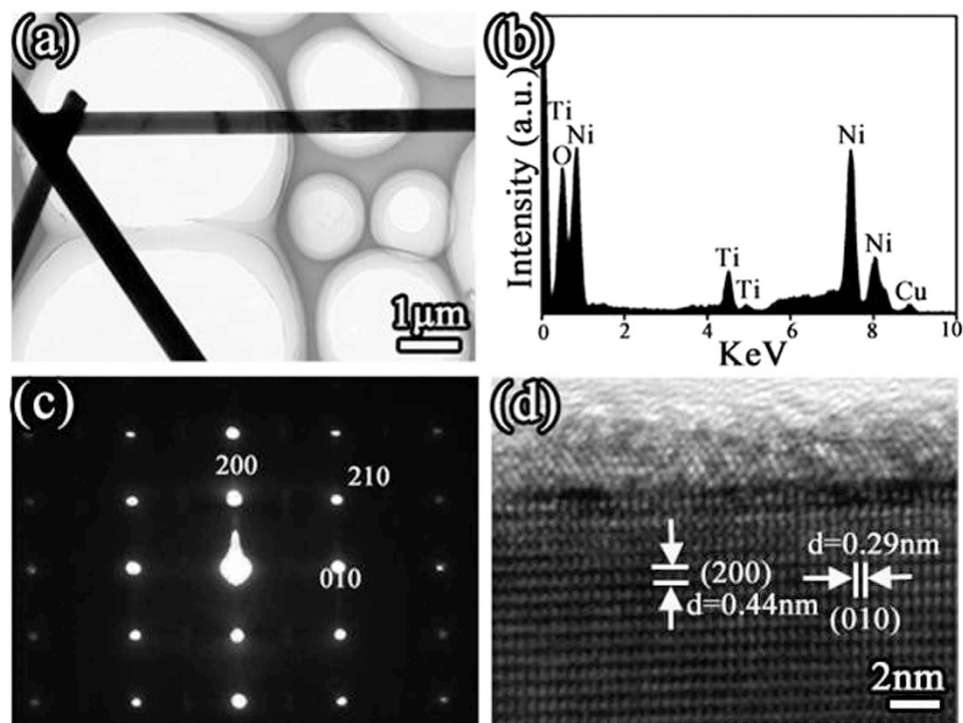


Figure 3. (a) representative TEM image of Ni_5TiO_7 nanowires by annealing PEO coating at 1050°C ; (b) EDS spectrum recorded from the nanowire; (c) SAED pattern taken from Ni_5TiO_7 nanowire and (d) its corresponding HRTEM image.

tailoring of Ni_5TiO_7 nanowires. In order to investigate the influence of Ni ion concentrations on the size and morphology evolution of Ni_5TiO_7 nanowires, the PEO coatings are dipped into $\text{Ni}(\text{NO}_3)_2$ solutions with a concentration of 0.1M, 0.5M and 2M for 1 hour, respectively. Figure 4 shows the typical morphology of Ni_5TiO_7 nanowires evolved from as-prepared PEO coating and pre-treated samples annealed at 1050°C for 1h. Notably, a significant difference in the morphology and size of Ni_5TiO_7 nanowires can be distinguished from these four samples. When the PEO coating is annealed without dipping into $\text{Ni}(\text{NO}_3)_2$ solution, only a small fraction of nanowires and nanoparticles with strip shapes and huge size can be found on its surface, as shown in Fig. 4a. XRD and EDS results (Supporting Information Figure S2) clearly demonstrate that the nanowires are Ni_5TiO_7 , suggesting that Ni ions in the electrolyte has been absorbed/stored in the PEO coating during arc-discharging process and further reacted with Ti/TiO_2 to lead to the formation of Ni_5TiO_7 phase. Figure 4b–d show the SEM images of Ni_5TiO_7 nanowires corresponding to $\text{Ni}(\text{NO}_3)_2$ solution concentrations of 0.1M, 0.5M and 2M, respectively and annealed at 1050°C for 1 hour. It can be found that the dipping process has a significant effect on the morphology and size evolutions of the Ni_5TiO_7 nanowires. Apparently, impregnating the PEO coating with 0.1M $\text{Ni}(\text{NO}_3)_2$ solution results in the drastic size reduction of Ni_5TiO_7 nanowires from 2–5 μm for as-prepared one to an average diameter of 50 nm (Fig. 4b). Inset of Fig. 4b gives a clear morphology and dimension size of Ni_5TiO_7 nanowires protruding from the PEO coating surface. When the Ni concentration is increased to 0.5M, both the diameter and length of Ni_5TiO_7 nanowires have evolved to ~300 nm and ~10 μm correspondingly, as shown in Fig. 4c. Further increase of the Ni concentration to 2M directly induces the fast growth of Ni_5TiO_7 nanowires to an average diameter of 4 μm (Fig. 4d). All these SEM observations clearly demonstrate that the dipping process is of great significance in tailoring the morphology and general size of Ni_5TiO_7 nanowires. Consequently, the morphology and size of Ni_5TiO_7 nanowires can be correspondingly modified by controlling the concentrations of $\text{Ni}(\text{NO}_3)_2$ solution. It is reasonable to understand the morphology and size evolution of Ni_5TiO_7 nanowires as a dependence of $\text{Ni}(\text{NO}_3)_2$ solution concentrations. In the case of lower content of $\text{Ni}(\text{NO}_3)_2$ solution, a thin layer of $\text{Ni}(\text{NO}_3)_2$ or Ni will cover on the PEO coating surface and aggregate into small islands under high-temperature annealing. These tiny Ni-containing islands with higher surface energy are preferential nucleation sites for the initial nucleation of Ni_5TiO_7 phase and serve as the seeds for controlling their subsequent crystallization. It should be strengthened that the initial size of these Ni-containing nanoparticles is of crucial importance in dominating the size of Ni_5TiO_7 nanowires. With the concentration increase of the $\text{Ni}(\text{NO}_3)_2$ solution, more $\text{Ni}(\text{NO}_3)_2$ or Ni will be deposited on the PEO coating surface and will give rise to the corresponding thickness enhancement of Ni-containing film. As a result, the nanoislands evolved from the thin film will correspondingly possess a large size for guiding the nucleation and the growth of Ni_5TiO_7 nanowires. The same phenomenon and process can also be expected in the case of

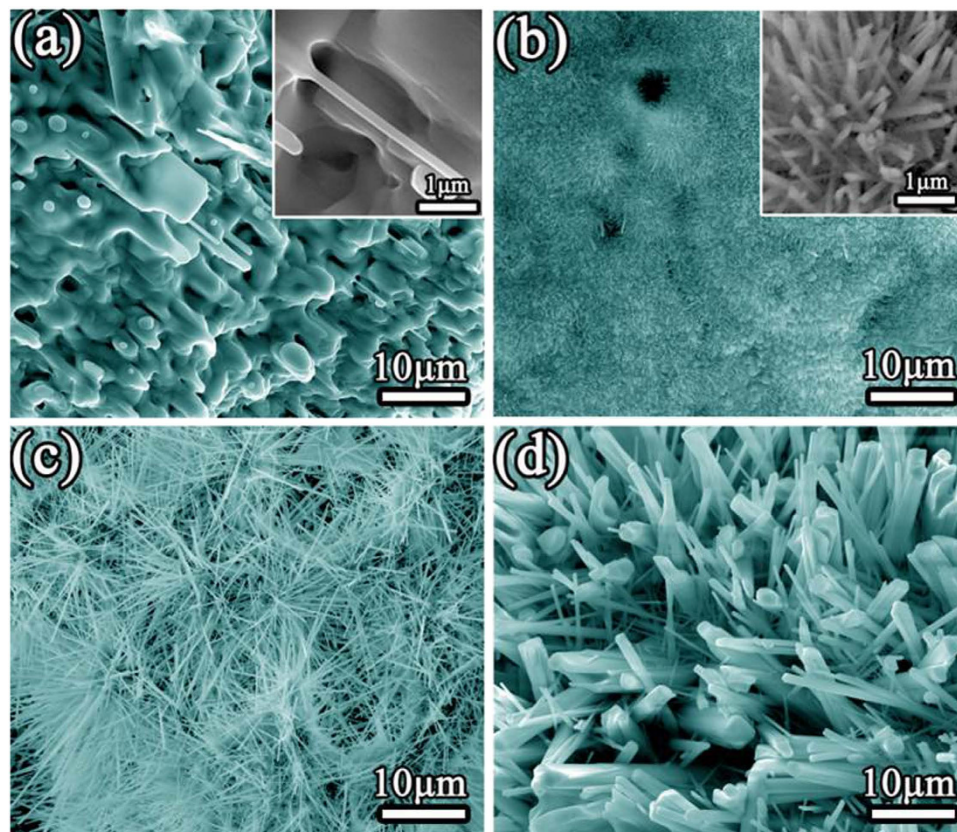


Figure 4. SEM morphologies of Ni_5TiO_7 nanowires grown on PEO coating in different $\text{Ni}(\text{NO}_3)_2$ concentrations of impregnation solutions at 1050°C : (a) without dipping; (b) 0.1 M; (c) 0.5 M and (d) 2 M.

2M $\text{Ni}(\text{NO}_3)_2$ solution for producing the largest size of Ni_5TiO_7 nanowires. The feasible size-controlling of Ni_5TiO_7 nanowires will undoubtedly provide more space for their catalytic performance tailoring and open up more opportunities for their applications.

Based on detailed SEM observations and TEM characterizations, a tentative reaction mechanism describing the formations of the PEO oxide coating and the Ni_5TiO_7 nanowires is proposed^{20,21}. At the first stage of PEO process, the titanium will be charged to Ti^{4+} ions and its surrounding aqueous solution (mainly H_2O) will be decomposed into H^+ and OH^- under high voltage and temperature, as described below²²:



Following this step, the Ti^{4+} will react with OH^- to lead to the formation of anatase and rutile TiO_2 phases under a huge temperature gradient generated by micro-arc discharge and aqueous cooling. The formation reaction of TiO_2 can be described as follows²³:



At the third stage of PEO process, $\text{Ni}(\text{CH}_3\text{COO})_2$ in the electrolyte can be ionized to Ni^{2+} and $(\text{CH}_3\text{COO})^-$ by the energetic arc discharge. The Ni^{2+} ions will react with other ions such as Ti^{4+} and OH^- under high temperature and high voltage, which leads to the formation of Ni-containing phase (like amorphous Ni_5TiO_7) in the PEO coating, similar to the formation of CaTiO_3 produced by the PEO method^{24,25}. It should be noted that the assertion of the formation of amorphous Ni-containing phase can be deduced from the dome peak in the XRD pattern (Fig. 1), which results from the repeatedly heating and cooling processes under high surface temperature produced by the micro-arc discharge in the electrolytic solution²⁶. It has been reported that the momentary temperature in the local discharge zones can be up to 4000~8000 K in a short time²⁶. When the PEO coating is subject to a high-temperature annealing at 1050°C , the Ni-contained amorphous phase will crystallize and the other excessive Ni ions

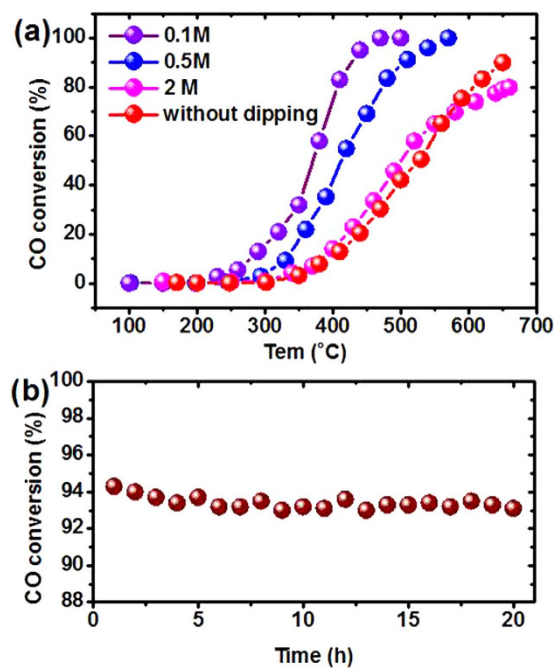


Figure 5. (a) Temperature-dependent CO catalytic oxidation performance over Ni_5TiO_7 nanowires catalysts prepared in different concentrations of impregnating solution; (b) the long-term stability test of Ni_5TiO_7 nanowires at 440 °C.

involved in the porous coating layer will diffuse into the top layer to provide Ni precursor and participate in the reaction with Ti/TiO₂ and oxygen. Finally, Ni_5TiO_7 nanostructures with high density can be achieved.

Previous study has demonstrated the outstanding performance of Ni_5TiO_7 catalysts in tar conversion with naphthalene as the target sample¹⁸. For considering its potential application in car exhaust processing, the CO oxidation over the as-prepared Ni_5TiO_7 nanowires is also evaluated. In order to characterize the “real” catalytic performance of the catalysts, Ni_5TiO_7 nanowires attached on TiO₂ coatings are peeled off from the Ti substrate. On the other hand, the Ni_5TiO_7 nanowires in the areas with uniform morphology and high growth density are used for the CO evaluation test in order to depress the influence of porous TiO₂ coating to the greatest extent. Figure 5a summarizes the CO conversion rate as a dependence of reaction temperature for all $\text{Ni}_5\text{TiO}_7/\text{TiO}_2$ composite catalysts prepared under different concentrations of $\text{Ni}(\text{NO}_3)_2$ solutions. It is noticed that the Ni_5TiO_7 nanowires corresponding to a 0.1M $\text{Ni}(\text{NO}_3)_2$ solution exhibit the best CO conversion capability in comparison with the other samples. Considering the morphology or growth density dependence on the concentration of $\text{Ni}(\text{NO}_3)_2$ solution, it is found that the Ni_5TiO_7 nanowires corresponding to 0.1M $\text{Ni}(\text{NO}_3)_2$ solution have the smallest nanowire size and largest growth density than the other samples, indicating that the CO conversion efficiency of Ni_5TiO_7 nanowires depends strongly on their size and growth density (Fig. 4). From Fig. 5a, it can be seen that the start temperature for CO conversion for Ni_5TiO_7 nanowires in the case of 0.1M $\text{Ni}(\text{NO}_3)_2$ solution is around 230 °C. This critical conversion temperature is still higher than that of metal or metal oxide like NiO/Au²⁷, Pt/CeO₂², but it should be kept in mind that the catalytic reaction of Ni_5TiO_7 nanowires is performed without any assistance of highly efficient noble metal catalysts. When the reaction temperature is increased to 440 °C, the CO oxidation capability is enhanced sharply and the catalytic activity approaches to the maximum. Almost all the CO has been completely converted into CO₂. For Ni_5TiO_7 nanowires corresponding to a $\text{Ni}(\text{NO}_3)_2$ concentration of 0.5 M, they exhibit the second best catalytic performance in all the four samples, which shows a starting reaction temperature at 300 °C and an end conversion temperature at 550 °C. However, the Ni_5TiO_7 nanowires corresponding to 2M $\text{Ni}(\text{NO}_3)_2$ solution show quite similar/comparable catalytic performance to the sample without any dipping. The significant difference in catalytic performance undoubtedly comes from the discrepancy of Ni_5TiO_7 nanowires in size and growth density, which provides different active sites for CO catalytic reaction. From above results, it can be concluded that the catalytic properties of Ni_5TiO_7 nanowires have close relation to their morphology and surface. SEM observation shown in Fig. 4 has demonstrated that increasing the concentrations of $\text{Ni}(\text{NO}_3)_2$ solutions can lead to their size increase correspondingly, directly resulting in the weakening of the CO conversion rate and performance. Like most metal oxide catalysts, the CO catalytic oxidation of Ni_5TiO_7 nanowires is closely related to nanowire size, the exposed surface area, mean diameter and the contact structure between the catalyst and the support metal oxides²⁸. It is believed that the desorption of CO and O₂ on the surface of Ni_5TiO_7 nanowires will react each other on the effect of Ni-O bonds and

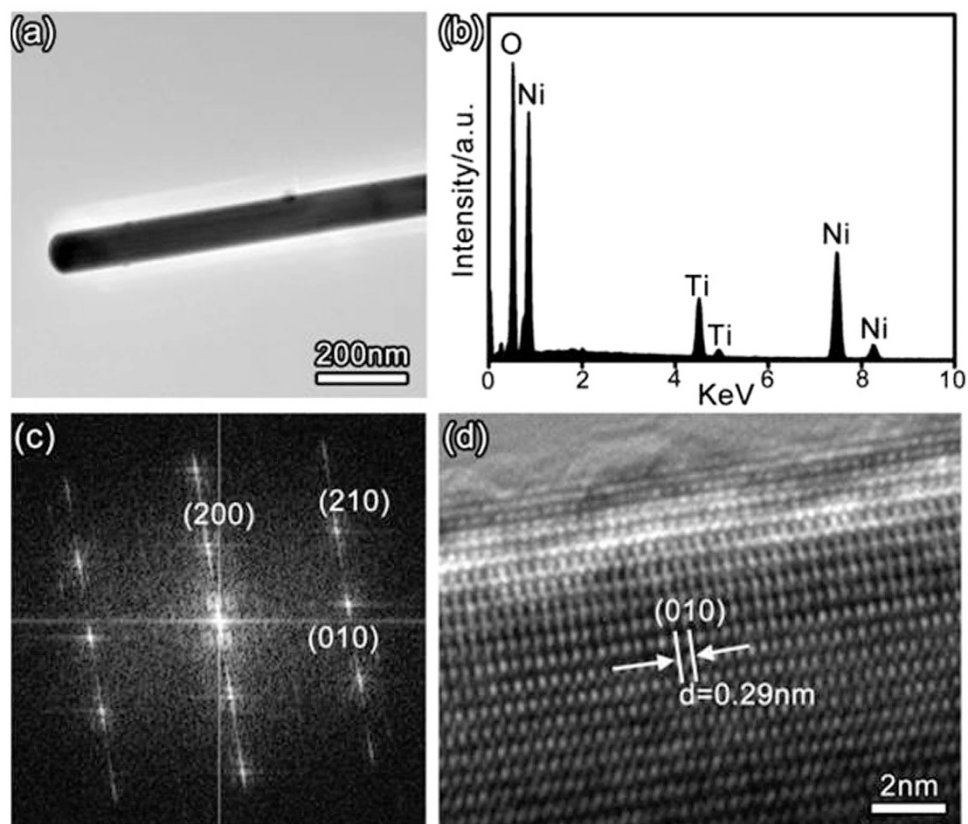


Figure 6. (a) Representative TEM image of Ni_5TiO_7 nanowires after CO catalytic oxidation; (b) EDS spectrum recorded from the nanowire; (c) FFT pattern taken from Ni_5TiO_7 nanowire and (d) its corresponding HRTEM image.

results in the catalytic oxidation²⁹. In addition, the evaluation of the long-term stability of Ni_5TiO_7 nanowires is also carried out. Figure 5b shows the continuous CO conversion test curve of Ni_5TiO_7 nanowires, which is annealed at 1050 °C and corresponding to a 0.1M $\text{Ni}(\text{NO}_3)_2$ solution. The long-term stability test is carried out at 440 °C since it shows the best activity in CO oxidation (Fig. 5a). Notably, the Ni_5TiO_7 nanowires exhibit extremely stable catalytic performance and no degradation of CO conversion efficiency is observed in the 20-hour test, further demonstrating the excellent high-temperature adaptation ability and thus it can be compared with some metal oxide catalysts like Co_3O_4 and NiCo_2O_4 ^{30,31}.

To comprehensively evaluate the application potential of Ni_5TiO_7 nanowire catalysts, the structural stability of Ni_5TiO_7 nanowires after several cycle high-temperature catalysis tests is investigated. The Ni_5TiO_7 nanowires continuously working at 440 °C for 20 hours are used as the samples for structure and crystallinity evaluations using TEM, as shown in Fig. 6. It is found that the morphology and appearance of the nanowires are not destroyed after the catalytic reaction (Fig. 6a). The nanowires still maintain their initial surface smoothness as the one shown in Fig. 3a. Further TEM observation on high-magnifications reveals that the nanowires still show superior crystallinity and the ordering of atoms is not deteriorated (Fig. 6d). Especially, the outer surface of the Ni_5TiO_7 nanowires still keeps the same feature as the one before catalytic reaction. Absence of any nanoparticles on the nanowire surface implies that the nanowires are not decomposed or involved into any phase transition reactions. Additionally, we do not observe any clues that verify the formation of polycrystalline or amorphous phases in the Fast Fourier Transition (FFT) (Fig. 6c). Composition analysis using high-resolution EDS confirms the same constitutions as the as-synthesized nanowires before catalytic reaction and impurity peaks from any possible phases are not found (Fig. 6b), further demonstrating the chemical stability of our nanowires involved in the CO oxidation. Apart from these merits, it should be strengthened that the Ni_5TiO_7 nanowires are *in-situ* fabricated on porous TiO_2 surface with improved substrate adherence. This peculiar advantage will in turn promote their direct fabrications on honeycomb-like metal substrate using PEO method and accelerate their practical utilization. With its predominant advantages in low-cost and easy synthesis process, as well as the superior performance in CO conversion and biomass gasification, the Ni_5TiO_7 nanowires will certainly open up more space as an efficient and chemically/structurally stable catalyst for environment-friendly applications ranging from car exhaust processing to chemical pollutant cleaning.

Conclusion

In summary, Ni₅TiO₇ nanowires with single crystal feature have been synthesized using conventional PEO method with subsequent impregnation and annealing processes. The size of Ni₅TiO₇ nanowires can be selectively tailored through simply controlling the Ni(NO₃)₂ concentration in dipping solution and an average minimized diameter as small as 50 nm can be obtained. CO oxidation tests demonstrates that the catalytic performance of Ni₅TiO₇ nanowires is strongly dependent on their size and growth density and the Ni₅TiO₇ nanowires with an average diameter of 50 nm show the best CO conversion efficiency. Long-term catalytic evaluation with a total reaction time of 20 hours and the precise HRTEM analysis verify the superior stability in catalytic performance and microstructure, which allows the current Ni₅TiO₇ nanowires as promising catalysts for diverse applications ranging from biomass gasification to car exhaust process.

Experimental Section

Samples preparation. Commercially available pure grade I titanium sheets (10 mm × 10 mm × 1 mm, Shanxi Baotai group) and graphite were connected to the positive and negative poles of power supply as anode and cathode, respectively. Titanium sheets are also used as the substrates to form porous TiO₂ coatings and the Ti precursor. Before the PEO process, the Ti substrates are ground using #1000 sand paper to remove the contaminated surface (TiO₂ or other impurity) and are cleaned with acetone, ethyl alcohol and distilled water. To promote the PEO process, mixed solutions comprising of sodium phosphate (Na₃PO₄·12H₂O, merck), sodium borate (Na₂B₄O₇·10H₂O, Merck), sodium tungstate (Na₂WO₄·2H₂O, Merck) and nickel acetate (Ni(CH₃COO)₂·4H₂O, Merck) are stored in a plastic box and are utilized as electrolytes and Ni precursors. It has been reported that PO₄³⁻, WO₄²⁻ and B₄O₇²⁻ ions can promote a uniform micro-arc generation, which is essential for producing homogeneous PEO coating^{32,33}. A detailed experimental setup for the PEO reaction can be found in Figure S3. The PEO process was carried out in a fixed applied current density mode of 0.1 A cm⁻². Other parameters including PEO time and pulse frequency were set at 10 min and 1000 Hz, respectively, for all samples after several rounds optimization. The electrolyte temperature was controlled under 50 °C for a full PEO reaction through circulating water cooling system during the PEO process. After the completion of the porous PEO coating, it was dipped into Ni(NO₃)₂ solutions with different concentrations for 1 hour for improving the Ni ion concentrations in the PEO coating. Following this step, the PEO coating were transferred to a resistance furnace for thermal annealing to promote the nucleation and crystallization of Ni₅TiO₇ catalysts. After maintaining the reaction at 1050 °C for 1 hour, high density of Ni₅TiO₇ nanostructures featured with a wire-like morphology on the surface of PEO coating were obtained.

Structure and composition characterization. Phase identification of the PEO coating and Ni₅TiO₇ nanostructures was examined by an X-ray diffractions (XRD, Rigaku D/max 2400) using CuK_α (λ_{Kα} = 0.154056 nm) as the x-ray source over a 2θ angle of 20–60°. The morphology of the coatings and Ni₅TiO₇ nanostructures are characterized by a field-emission scanning electron microscopy (FE-SEM, FEI Inspect F50) equipped with a Quanta 600 Energy Dispersed X-ray spectrometer (EDS) system. The microstructure, crystallinity and elemental compositions of Ni₅TiO₇ nanowires scratched from the coating surfaces were characterized by a transmission electron microscopy (TEM, Tecnai, F20) under an accelerated voltage of 200 kV.

Catalytic tests. All the catalytic activity evaluations of Ni₅TiO₇/TiO₂ composite catalysts for CO oxidation were carried out by using a fixed-bed quartz tubular reactor. The catalysts peeled off from the Ti substrate were placed in the active zone of the quartz tubular reactor. Mixed gases (1.0% CO, 10% O₂, balanced with helium) are transported into the reactor at a flowing rate of 10 ml/min. The reactants and products were analyzed by using an on-line gas chromatography system (Agilent 7890A) with a molecular sieve column. CO and CO₂ gases were detected with a thermal conductivity detector. All the catalytic tests were carried out at the temperatures ranging from 25 °C to 650 °C.

References

- Shelif, M. & McCabe, R. W. Twenty-five years after introduction of automotive catalysts: what next? *Catal. Today* **62**, 35–50 (2000).
- Bera, P., Patil, K. C., Jayaram, V., Subbanna, G. N. & Hegde, M. S. Ionic Dispersion of Pt and Pd on CeO₂ by Combustion Method: Effect of Metal–Ceria Interaction on Catalytic Activities for NO Reduction and CO and Hydrocarbon Oxidation. *J Catal* **196**, 293–301 (2000).
- Saberi, M. H., Mortazavi, Y. & Khodadadi, A. A. Dual selective Pt/SnO₂ sensor to CO and propane in exhaust gases of gasoline engines using Pt/LaFeO₃ filter. *Sens. Actuators B: Chem.* **206**, 617–623 (2015).
- Remediakis, I. N., Lopez, N. & Nørskov, J. K. CO Oxidation on Rutile-Supported Au Nanoparticles. *Angew. Chem.* **117**, 1858–1826 (2005).
- Laguna, O. H., Hernandez, W. Y., Arzamendi, G., Gandia, L. M., Centeno, M. A. & Odriozola, J. A. Gold supported on CuOx/CeO₂ catalyst for the purification of hydrogen by the CO preferential oxidation reaction (PROX). *Fuel* **118**, 176–185 (2014).
- Cao, J. L., Wang, Y., Zhang, T. Y., Wu, S. H. & Yuan, Z. Y. Preparation, characterization and catalytic behavior of nanostructured mesoporous CuO/Ce_{0.8}Zr_{0.2}O₂ catalysts for low-temperature CO oxidation. *Appl Catal B-environ* **78**, 120–128 (2008).

7. Wu, Z. W. *et al.* Preferential oxidation of CO in H₂-rich stream over CuO/Ce_{1-x}Ti_xO₂ catalysts. *Appl Catal B: Environl* **98**, 204–212 (2010).
8. Zou, Z. Q., Meng, M., Guo, L. H. & Zha, Y. Q. Synthesis and characterization of CuO/Ce_{1-x}Ti_xO₂ catalysts used for low-temperature CO oxidation. *J Hazard Mater* **163**, 835–842 (2009).
9. Konova, P., Stoyanova, M., Naydenov, A., Christoskova, S. & Mehandjiev, D. Catalytic oxidation of VOCs and CO by ozone over alumina supported cobalt oxide. *Appl Catal A: Gen* **298**, 109–114 (2006).
10. Liu, S. Q., Tang, Z.-R., Sun, Y. G., Colmenare, Juan Carlos & Xu, Y.-J. One-dimension-based spatially ordered architectures for solar energy conversion. *Chem Soc Rev* **44**, 5053–5075 (2015).
11. Weng, B. S., Liu, S. Q., Tang, Z.-R. & Xu, Y.-J. One-dimensional nanostructure based materials for versatile photocatalytic applications. *RSC Adv* **4**, 12685–12700 (2014).
12. Yoshida, S. *et al.* Analysis of xanes for identification of highly dispersed transition metal oxides on supports. *Catal Lett.* **12**, 277–286 (1992).
13. Chang, X. T., Sun, S. B., Xu, X. & Li, S. J. Synthesis of transition metal-doped tungsten oxide nanostructures and their optical properties. *Mater Lett* **65**, 1710–1712 (2011).
14. Sriwong, P., Thongtem, T., Phuruangrat, A. & Thongtem, S. Hydrothermal synthesis, characterization, and optical properties of wolframite ZnWO₄ nanorods. *CrystEngComm* **13**, 1564–1569 (2011).
15. Patcas, F. & Krysmann, W. Efficient catalysts with controlled porous structure obtained by anodic oxidation under spark-discharge. *Appl Catal A: Gen* **316**, 240–249 (2007).
16. Bayati, M. R., Molaie, R., Moshfegh, A. Z., Golestani-Fard F. A strategy for single-step elaboration of V₂O₅-grafted TiO₂ nanostructured photocatalysts with evenly distributed pores. *J Alloys Compd.* **509**, 6236–6241 (2011).
17. Shimura, F. & Kawamura, T. Crystal-Growth of a New Phase Ni₅TiO₇ and Its Crystallographic Properties. *Jpn J Appl Phys* **15**, 1403–1404 (1976).
18. Jiang, X. *et al.* Highly efficient nanoarchitected Ni₅TiO₇ catalyst for biomass gasification. *ACS Appl Mater & Inter* **4**, 4062–4066 (2012).
19. Tong, W. M. *et al.* Kinetic Control of MnWO₄ Nanoparticles for Tailored Structural Properties. *J. Phys. Chem. C* **114**, 15298–15305 (2010).
20. Bayati, M. R., Moshfegh, A. Z. & Golestani-Fard, F. Synthesis of narrow band gap (V₂O₅)_x-(TiO₂)_{1-x} nano-structured layers via micro arc oxidation. *Appl Surf Sci* **256**, 2903–2909 (2010).
21. Yerokhin, A. L., Nie, X., Leyland, A., Matthews, A. & Dowey, S. J. Plasam electrolysis for surface engineering. *Surf Coat Technol* **122**, 73–93 (1999).
22. Sarbishei, S., Sani, M. A. F. & Mohammadi, M. R. Study plasma electrolytic oxidation process and characterization of coatings formed in an alumina nanoparticle suspension. *Vacuum* **108**, 12–19 (2014).
23. Bayati, M. R., Golestani-Fard, F. & Moshfegh, A. Z. Photo-Degradation of Methylene Blue over V₂O₅-TiO₂ Nano-Porous Layers Synthesized by Micro Arc Oxidation. *Catal Lett* **134**, 162–168 (2009).
24. Yerokhin, A. L., Nie, X., Leyland, A. & Matthews, A. Characterisation of oxide films produced by plasma electrolytic oxidation of a Ti-6Al-4V alloy. *Surf Coat Technol* **130**, 195–206 (2000).
25. Durdu, S., Deniz, Ö. F., Kutbay, I. & Usta, M. Characterization and formation of hydroxyapatite on Ti6Al4V coated by plasma electrolytic oxidation. *J Alloy Compd.* **551**, 422–429 (2013).
26. Albella, J. M., Montero, I. & Martinez-Duant, J. M. Electron injection and avalanche during the anodic oxidation of tantalum. *Solid-State Sci and Techn.* **131**, 1101–1104 (1984).
27. Xu, X. J., Fu, Q., Guo, X. G. & Bao, X. H. A highly active "NiO-on-Au" Surface Architecture for CO Oxidation. *ACS Catal.* **3**, 1810–1818 (2013).
28. Bamwenda, G. R., Tsubota, S., Nakamura, T. & Haruta, M. The influence of the preparation methods on the catalytic activity of platinum and gold supported TiO₂ for CO oxidation. *Catal Lett* **44**, 83–87 (1997).
29. Mahammadunnisa, S., Manoj Kumar Reddy, P., Lingaiah, N. & Subrahmanyam, C. NiO/Ce_{1-x}Ni_xO_{2-δ} as an alternative to noble metal catalysts for CO oxidation. *Catal. Sci. Technol* **3**, 730–736 (2013).
30. Grillo, F., Natile, M. M. & Glisenti, A. Low temperature oxidation of carbon monoxide: the influence of water and oxygen on the reactivity of a Co₃O₄ powder surface. *Appl Catal B: Environ* **48**, 267–274 (2004).
31. Ren, Z. *et al.* Monolithically Integrated Spinel M_xCo_{3-x}O₄ (M=Co, Ni, Zn) Nanoarray Catalysts: Scalable Synthesis and Cation Manipulation for Tunable Low-Temperature CH₄ and CO Oxidation. *Angew Chem Int Edit* **53**, 7223–7227 (2014).
32. Liang, J., Srinivasan, P. B., Blawert, C., Störmer, M. & Dietzel, W. Electrochemical corrosion behaviour of plasma electrolytic oxidation coatings on AM50 magnesium alloy formed in silicate and phosphate based electrolytes. *Electrochim Acta* **54**, 3842–3850 (2009).
33. Zheng, H. Y., Wang, Y. K., Li, B. S. & Han, G. R. The effects of Na₂WO₄ concentration on the properties of microarc oxidation coatings on aluminum alloy. *Mater Lett* **59**, 139–142 (2005).

Acknowledgments

This work was financially supported by the Knowledge Innovation Program of Institute of Metal Research (IMR), Chinese Academy of Science (CAS) (grants No. Y2NCA111A1, Y3NCA111A1) and the Youth Innovation Promotion Association, Chinese Academy of Sciences (Grant No. Y4NC711171).

Author Contributions

B.D.Liu and X.Jiang designed the experiment. Y.N.Jiang, X.Y.Liu, C.Weimer and L.S.Liu carried out the growth experiment. B.Yang performed all TEM analyses. L.N.Yang carried out the catalytic test. Y.N.Jiang, B.D.Liu and X.Jiang co-wrote the manuscript.

Additional Information

Supplementary information: accompanies this paper at <http://www.nature.com/srep>

Competing financial interests: The authors declare no competing financial interests.

How to cite this article: Jiang, Y. *et al.* Size-controllable Ni₅TiO₇ nanowires as promising catalysts for CO oxidation. *Sci. Rep.* **5**, 14330; doi: 10.1038/srep14330 (2015).



This work is licensed under a Creative Commons Attribution 4.0 International License. The images or other third party material in this article are included in the article's Creative Commons license, unless indicated otherwise in the credit line; if the material is not included under the Creative Commons license, users will need to obtain permission from the license holder to reproduce the material. To view a copy of this license, visit <http://creativecommons.org/licenses/by/4.0/>